

# Dynamic Mechanical and Thermal Analyses of Magnetic Particle and Metal Evaporated Tapes and Their Individual Layers

Tiejun Ma, Bharat Bhushan

*Nanotribology Laboratory for Information Storage and MEMS/NEMS, The Ohio State University, 206 W. 18th Avenue, Columbus, Ohio 43210*

Received 14 August 2002; accepted 30 September 2002

**ABSTRACT:** The mechanical and thermal properties of magnetic tapes and their individual layers strongly affect the tribology of the magnetic head–tape interface. Dynamic mechanical analysis and thermomechanical analysis tests were performed on magnetic tapes, tapes with front coat or back coat removed, substrates (with front and back coats removed), and never-coated virgin films of the substrates. Storage modulus and loss tangent were obtained at a frequency range from 0.016 to 28 Hz, and at a temperature range from −50 to 150 or 210°C. Coefficients of thermal expansion (CTE) of various samples were measured at a temperature range from 30 to 70°C. The tapes used in this research include two magnetic particle (MP) tapes and two metal evaporated (ME) tapes based on poly(ethylene terephthalate) and poly(ethylene naphthalate) substrates. The master curves of storage modulus for these samples were generated for a frequency range from  $10^{-20}$  to  $10^{15}$  Hz. The effect of the tape manufacturing process on the dynamic

mechanical properties of substrates was analyzed by comparing the data for the substrates (with front and back coats removed) and the never-coated virgin films. A model based on the rule of mixtures was developed to determine the storage modulus, complex modulus, and CTE for the front coat and back coat of MP and ME tapes. To validate the procedure, data for these individual layers were then used to calculate the corresponding properties of the finished tape. The predicted results were compared with the experimental measurements. The data obtained in the study are also discussed in light of previously published lateral contraction, Poisson's ratio, CTE, and CHE (coefficient of hygroscopic expansion) data. © 2003 Wiley Periodicals, Inc. *J Appl Polym Sci* 89: 548–567, 2003

**Key words:** magnetic tape; rule of mixtures; storage modulus; mechanical properties; CTE

## INTRODUCTION

Magnetic tapes, compared to other storage media, provide extremely high volumetric density, high data rates, and low cost per megabyte. These are primarily used for data backup and some high volume recording devices such as instrument and satellite recorders.<sup>1</sup> For example, the Generation 4 Ultrium format LTO (linear tape open) tape provides for up to 1.6 TB in a single cartridge, with a compressed-data rate of up to 320 MB s<sup>−1</sup>.<sup>2</sup> The high volumetric density is achieved by a combination of high areal density and the use of an ultrathin tape. This requires that the substrate and the finished tape be mechanically and environmentally stable in both the longitudinal (for high linear density) and lateral (for high track density)

directions. Ever increasing recording density requires a better understanding of the dimensional stability of the tape, especially of the polymeric substrate, which takes 75 to 95% of the total thickness. As a way to minimize stretching and damage during manufacturing and use of thin magnetic tapes, the substrate should be a high modulus, high strength material with low viscoelastic and shrinkage characteristics. Moreover, because high coercivity magnetic films on metal evaporated (ME) tapes are deposited and heat treated at elevated temperatures, an ME substrate with stable mechanical properties up to a temperature of 100–150°C or even higher is desirable.<sup>1</sup>

The second author's group has extensively studied the viscoelastic properties and dimensional stability of ultrathin polymeric films and tapes.<sup>1,3–8</sup> This includes the creep, shrinkage, dynamic mechanical behavior, Poisson's ratio, and both thermal and hygroscopic expansion of polymeric substrates, tapes, and stripped tapes without front coat and/or back coat. Weick and Bhushan<sup>5,6</sup> modeled the magnetic tape as a three-layer composite consisting of front coat, substrate, and back coat. By performing the creep tests on the combined layers and applying the rule of mixtures, the creep

Correspondence to: B. Bhushan (bhushan.2@osu.edu).

Contract grant sponsor: Nanotribology Laboratory for Information Storage and MEMS/NEMS (NLIM), The Ohio State University.

Contract grant sponsor: Teijin-DuPont Ltd. Japan.

Contract grant sponsor: DuPont-Teijin Ltd.

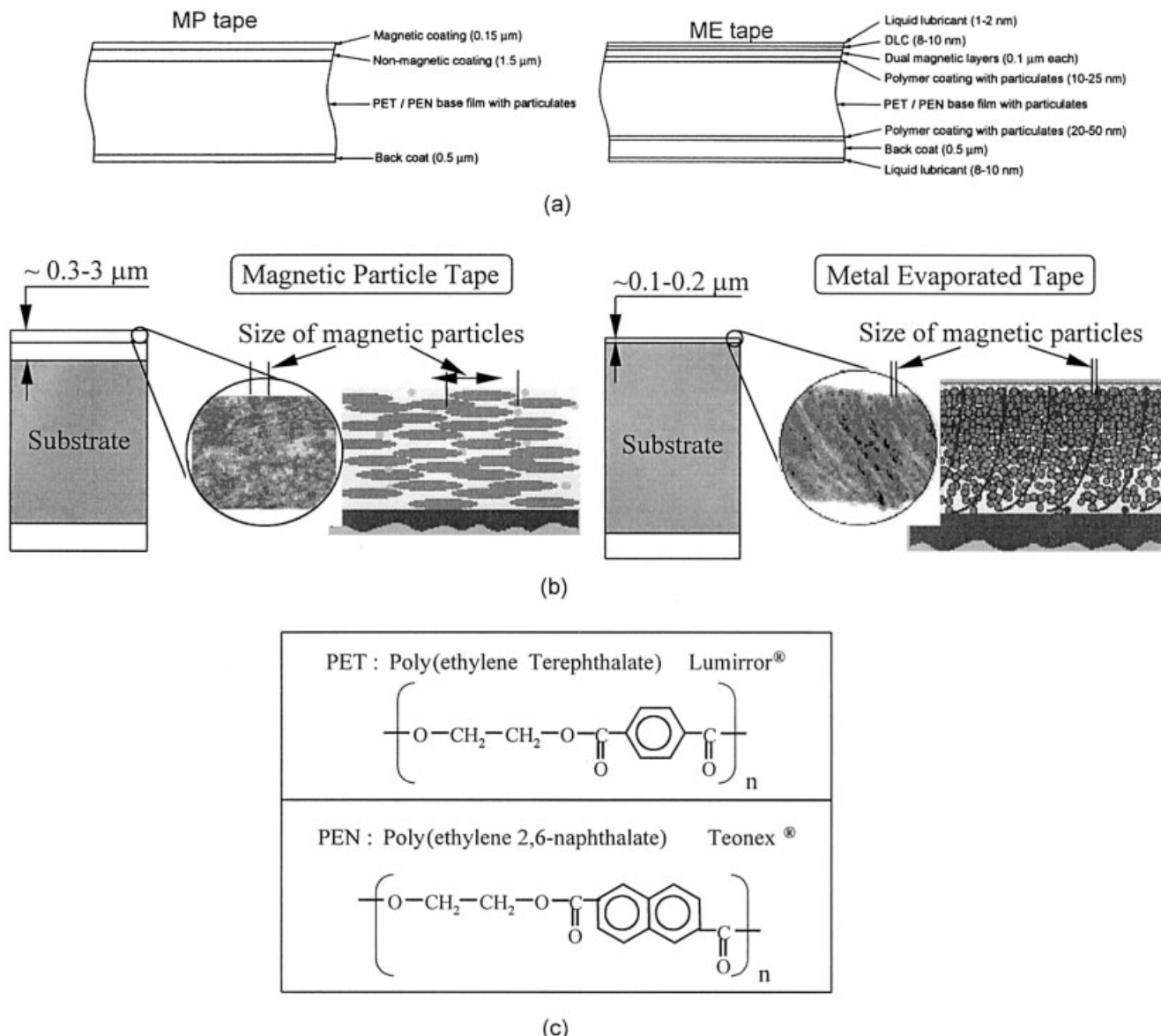


**Figure 1** Magnetic tape: (a) Schematic diagram of MP and ME tapes, (b) detailed construction of MP and ME tapes (downloaded from ref. 2, and slightly modified), (c) chemical unit structures of various polymeric films.

compliance of each individual layer was obtained. Additionally, the strain distribution was predicted through the thickness of the tape. Ma and Bhushan<sup>9,10</sup> developed a technique to measure and calculate the lateral contraction of magnetic tapes and their individual layers. However, the dynamic mechanical and thermal mechanical properties for these layers are still not available. There is another key concern to tape and substrate manufacturers, the degradation of the substrate during tape manufacturing, which has not been reported. Such information is useful for designers wanting to develop future magnetic tapes that utilize thinner and highly stable materials.

The main objective of this study was to measure and calculate the dynamic mechanical properties (storage modulus and loss tangent) and coefficient of thermal

expansion (CTE) of magnetic tapes and their individual layers, as well as to study the effect of the tape manufacturing processing on the dynamic mechanical properties of substrates. Two magnetic particle (MP) tapes and two ME tapes, each of which use two typical polyester substrates [poly(ethylene terephthalate) (PET) and poly(ethylene naphthalate) (PEN)], and corresponding never-coated virgin films, were studied.

## EXPERIMENTAL

### Test samples

Magnetic tapes selected for this study are shown in Figure 1(a) and (b). These tapes are representative of the two basic types of MP tapes in which magnetic

TABLE I  
Sample Matrix: Symbols and Thickness ( $\mu\text{m}$ )

Width (mm)	Tape	Substrate + front coat	Substrate + back coat	Substrate	Never-coated substrate film <sup>a</sup>
12.67	MP-DLT 8.9	MP-DLT/SF ~ 8.6	MP-DLT/SB ~ 6.5	MP-DLT/S 6.1	T-PET(2) 6.1
12.67	MP-LTO 8.9			MP-LTO/S 6.1	T-PEN 6.1
8	ME-Hi8 10.46	ME-Hi8/SF ~ 10.06	ME-Hi8/SB ~ 10.3	ME-Hi8/S 9.9	T-PET(3) 9.9
6.35	ME-MDV 5.26			ME-MDV/S 4.7	T-PEN(2) 4.7

<sup>a</sup> T-PEN corresponds to the sample in Refs. 7 and 8. T-PEN(2), T-PET(2), and T-PET(3) correspond to the sample in Ref. 10.

particles are dispersed in a polymeric binder; and ME tapes in which continuous films of magnetic materials are deposited onto the substrate using vacuum techniques. Both of the MP tapes used in this study, MP-DLT with 6.1  $\mu\text{m}$  PET substrate and MP-LTO with 6.2  $\mu\text{m}$  PEN substrate, had a total thickness of 8.9  $\mu\text{m}$ . The substrate for ME-Hi8 was 9.9  $\mu\text{m}$  thick PET, and that for ME-MDV was 4.7  $\mu\text{m}$  thick PEN.

PET and PEN films are commonly used as magnetic tape substrates, and have been widely studied.<sup>1,7,8,11</sup> Their chemical molecular structures are shown in Figure 1(c). The glass-transition temperatures ( $T_g$ ) for the PET and PEN substrates are about 80 and 120°C, respectively.<sup>8,11</sup> Typical crystallinities for PET and PEN films are about 40–50 and 30–40%, respectively.<sup>8</sup> Information about the specific chemistry of the materials used in the front and back coats is not available from the manufacturers. However, based on Bhushan,<sup>1</sup> the front coat may consist of a single magnetic layer, as in the cases of single-layer MP tapes. Their composite magnetic layers consist of magnetic particles, a polymer binder, and a lubricant. The MP tape magnetic layer also consists of abrasive (mostly alumina) and conductive carbon particles. The front coat may also consist of a magnetic layer and a nonmagnetic polymer underlayer, as in the case of double-layer MP tape. For ME tapes, the front coat consists of a magnetic layer, a diamond-like carbon (DLC) coating, and a lubricant layer. The ME tape magnetic layer is a continuous thin film of Co–Ni–O deposited by evaporation. The back coat consists of carbon black in a polymeric binder.

Symbols of the samples are listed in Table I, which include the following layer formats:

- Magnetic tapes as cut from the cassettes
- Substrates (front coat and back coat removed) (S)
- Substrate plus front coat (back coat removed) (SF)
- Substrate plus back coat (front coat removed) (SB)
- Never-coated virgin substrate film

To obtain the substrate for the MP tapes, methyl ethyl ketone (MEK) was used to remove the front and

back coats. This involved placing the tape on a flat piece of glass and rubbing both sides of the tape longitudinally with a paper towel saturated with MEK until only the transparent PET substrate remained. The substrate for the ME tape was obtained in a similar manner. However, MEK could be used to remove only the back coat of the ME tape. A 2% hydrochloric acid solution was used to remove the front coat. This procedure involved dipping the ME tape into the solution until the metal evaporated coating could be rubbed off.

Removing the back coat of the MP and ME tapes without removing the front coat involved spreading a thin bead of distilled water on a glass plate. The tape specimen was then placed front coat down in this bead of water. All excess water around the edges of the tape was soaked up with a paper towel. The back coat could then be carefully removed using MEK, and the thin film of polar water molecules between the glass plate and front coat of the tape helped prevent the nonpolar MEK molecules from dissolving the front coat. Removing the front coat on the MP and ME tapes without removing the back coat involved the same procedure. All samples were left in ambient conditions (24–26°C, 30–60% RH) for at least 4 days before testing.

## Test apparatus and procedure

### Dynamic mechanical analysis

An RSA II dynamic mechanical analyzer (Rheometrics, Piscataway, NJ) was used to measure the dynamic mechanical properties of the polymeric films.<sup>1,8</sup> Figure 2 shows the functional block diagram of this test apparatus. The analyzer was used in a tension/compression mode, and rectangular samples (6.35 mm wide  $\times$  22.5 mm long) were used. In this mode, rectangular samples were fastened vertically between the grips and a sinusoidal strain was applied to the specimen. Frequency/temperature sweep experiments were performed for a 0.1 to 182 rad  $\text{s}^{-1}$  (0.016–29 Hz) range, and 14 data points were taken for each fre-

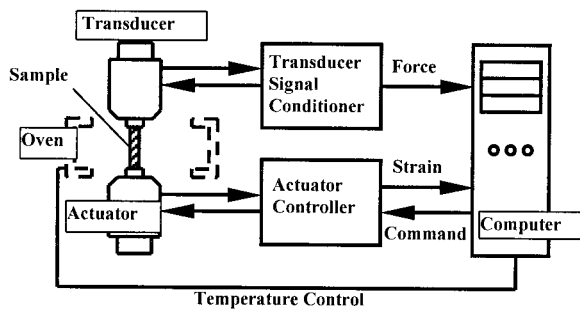


**Figure 2** Functional block diagram of DMA test apparatus (RSA II; Rheometrics, Piscataway, NJ).

quency sweep at 11 different temperature levels ranging from  $-50$  to  $150^{\circ}\text{C}$  for the PET films and corresponding tapes, and 14 temperature levels ranging from  $-50$  to  $210^{\circ}\text{C}$  for PEN films and corresponding tapes. The temperature increment was  $20^{\circ}\text{C}$ , and the soak time for each temperature level was 10 s. The test temperatures were selected to cover the glass-transition temperatures of the substrate films.

The analyzer was operated in "autotension" mode with a static force on the samples. This prevented buckling of the thin films by applying the peak dynamic forces (corresponding to a strain of 0.25%) while using the static force as a mean, as shown in Figure 3(a).<sup>12</sup> It was found that a static strain of more than 0.25% was needed to prevent buckling [see Fig. 3(b) for an example for Standard PET]. Therefore the initial static force of 80 g was used for MP-DLT and ME-Hi8 samples, and 65 and 40 g were used for MP-LTO and ME-MDV samples, respectively, which is equivalent to a strain offset of about 0.25%.

Equations used to calculate the storage (or elastic) modulus  $E'$  and loss tangent  $\tan \delta$  are as follows:

$$E' = \cos \delta \left[ \frac{\bar{\sigma}}{\varepsilon} \right] \quad (1)$$

$$E'' = \sin \delta \left[ \frac{\bar{\sigma}}{\varepsilon} \right] \quad (2)$$

$$|E^*| = \sqrt{(E')^2 + (E'')^2} \quad (3)$$

$$\tan \delta = \frac{E''}{E'} \quad (4)$$

$$\varepsilon = \frac{D}{L} \quad \sigma = FgK_{\sigma} \quad (5)$$

where  $E'$  is the storage modulus;  $E''$  is the loss (or viscous) modulus;  $|E^*|$  is the magnitude of the complex modulus;  $\varepsilon$  is the applied strain;  $\sigma$  is the measured stress;  $\delta$  is the measured phase angle shift between stress and strain;  $D$  is the displacement from the strain

transducer;  $L$  is the original length of the sample;  $K_{\sigma}$  is a stress constant equal to  $100/wt$ ,<sup>12</sup> where  $w$  is the width of the sample and  $t$  is the thickness of the sample;  $g$  is the gravitational constant ( $9.81 \text{ m s}^{-2}$ ); and  $F$  is the measured force on the sample from the load cell. The T-PET(2) sample was measured a number of times to check for the reproducibility. Reproducibility of  $E'$  and  $\tan \delta$  were about  $\pm 5$  and  $\pm 3\%$ , respectively.

### Thermomechanical analysis

The thermal expansion character of the samples was measured on a commercially available TMA instrument TA-2940 (TA Instruments, New Castle, DE).<sup>10</sup> The typical sample size was  $3 \times 40 \text{ mm}$  and after clipping, the gauge length of the sample was about 25.5 mm. For CTE measurement, the temperature ranged from 10 to  $70^{\circ}\text{C}$ , at a heating rate of  $3^{\circ}\text{C}/\text{min}$ . A constant 3-g force was applied to the sample to keep it flat and stable. Aluminum foil ( $15.4 \mu\text{m}$  thick, CTE =  $23.6 \times 10^{-6}/^{\circ}\text{C}$ ; Reynolds, Columbus, OH) was used to calibrate the instrument. Dimensional change

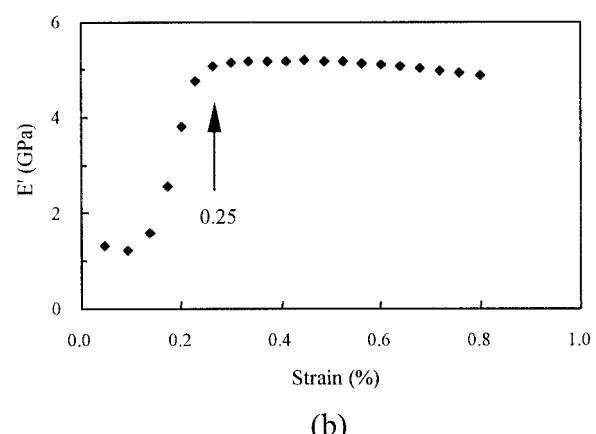
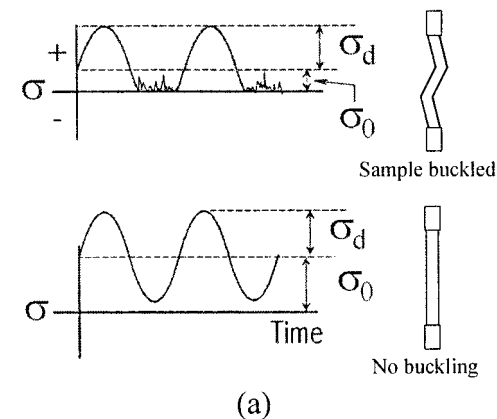


**Figure 3** (a) Schematic showing the effect of pretension (static force) on the sample buckling, and (b) an example of storage modulus ( $E'$ ) measurement in a strain-sweep test of a standard PET sample.  $E'$  remains steady after a strain of about 0.25%; sample buckles below this strain value.

(thermal expansion) of the sample was directly measured by the instrument, then it was converted to the CTE by the equation

$$\alpha = \frac{\Delta l}{l \Delta T} \quad (6)$$

where  $\Delta l$  and  $l$  are the change in length and original length at 30°C, and  $\Delta T$  is the temperature range. According to ASTM E831-93,<sup>13</sup> the measured CTE at the initial 20°C (10–30°C) was regarded as unstable, and was not used in the discussion in this study. The T-PEN sample was measured a number of times to check for reproducibility, which was within  $\pm 1.5 \times 10^{-6}/^{\circ}\text{C}$ .

### Atomic force microscopy

For rule of mixtures analysis, the thicknesses of various layers in the tapes were needed. Besides the substrates, only the thicknesses of two MP tapes were known before the experiments. Thus, an atomic force microscope (AFM, D3100; Digital Instruments, Santa Barbara, CA) was used to measure the thickness of the front and back coats.<sup>14</sup> The procedure is illustrated in Figure 4. In Figure 4(a), part of the front coat of the ME-Hi8 tape was removed, then an area across the boundary was imaged by AFM using a 5- to 10-nm radius silicon tip in the tapping mode. The scan size used was about  $75 \times 75 \mu\text{m}$  with  $256 \times 256$  pixels. Figure 4(b) shows the procedure for the measurement of the back coat of ME-Hi8 tape. An ink mark was made for identification of the selected boundary area. Using this methodology, the back coats of MP-DLT and MP-LTO, and the front and back coats of ME-Hi8 and ME-MDV tapes were measured.

### Rule of mixtures approach

Because magnetic tapes consist of multiple layers, they resemble polymer composite laminates.<sup>5,6,10</sup> Generally, they can be regarded as a three-layer composite, as shown in Figure 5. The rule of mixtures method can be used to predict the elastic mechanical properties of the whole tape if the data for each layer are known, assuming that there is perfect bonding between each layer, that is, assuming isostrain.<sup>15</sup> Based on this rule,

$$\sigma_t A_t = \sigma_f A_f + \sigma_s A_s + \sigma_b A_b \quad (7)$$

where  $\sigma_t$ ,  $\sigma_f$ ,  $\sigma_s$ , and  $\sigma_b$  are the stresses in the entire tape, front coat, substrate, and back coat, respectively; and  $A_t$ ,  $A_f$ ,  $A_s$ , and  $A_b$  are the cross-sectional areas of the tape, front coat, substrate, and back coat, respectively. Additionally,

$$E_t t = E_f f + E_s s + E_b b \quad (8)$$

where  $E_t$ ,  $E_f$ ,  $E_s$ , and  $E_b$  are the Young's moduli of the tape, front coat, substrate, and back coat, respectively; and  $t$ ,  $f$ ,  $s$ , and  $b$  are the thicknesses of the corresponding layers.

For any two combined layers, similar equations apply, such as

$$E_{fs}(f + s) = E_f f + E_s s \quad (9)$$

where  $E_{fs}$  is the Young's modulus of the combined layers of substrate plus front coat.

If we know two of the moduli in eq. (9), for example,  $E_{fs}$  and  $E_s$ , and the thickness of each layer, we can calculate the third modulus, say  $E_f$ ,

## RESULTS AND DISCUSSION

### Thickness of individual layer of the tapes

Based on AFM measurements, the two ME tapes were found to have similar front coat and back coat thicknesses, 0.16 and 0.4  $\mu\text{m}$ , respectively. The thicknesses of back coats of MP tapes are about 0.4  $\mu\text{m}$  (MP-DLT) and 0.3  $\mu\text{m}$  (MP-LTO). The thicknesses of various layers of magnetic tapes are listed in Table I.

### DMA results

The storage modulus and loss tangent as a function of frequency and temperature for various materials are shown in Figure 6(a)–(f). High storage modulus indicates high elastic stiffness. From the three-dimensional surface representations of storage modulus, it can be seen that higher elastic moduli correspond to higher deformation frequencies and lower temperatures. High loss tangent indicates more viscoelastic behavior of the material, or more energy is dissipated during the deformation. For a general comparison, Table II summarizes the storage moduli of various samples at 0.016 and 28 Hz, 25°C.

In Figure 6(a), the storage moduli of the five MP-DLT samples have a similar tendency, that is, the rate of decrease of storage moduli as a function of temperature is low before it reaches to about 70°C; the rate then suddenly increases and storage moduli drop to a low level, as the material transits from a glassy to a rubbery state. This change corresponds to the character of the loss tangents in Figure 6(b), where the loss tangent remains low (below 70°C), indicating that a small amount of energy is dissipated; the loss tangent then begins to rise at 70–90°C and peaks at 110–130°C. These tendencies and critical temperatures are identical to all the MP-DLT samples, including tape, combined layers, substrate, and the virgin film T-PET(2). This demonstrates that the dynamic mechanical prop-

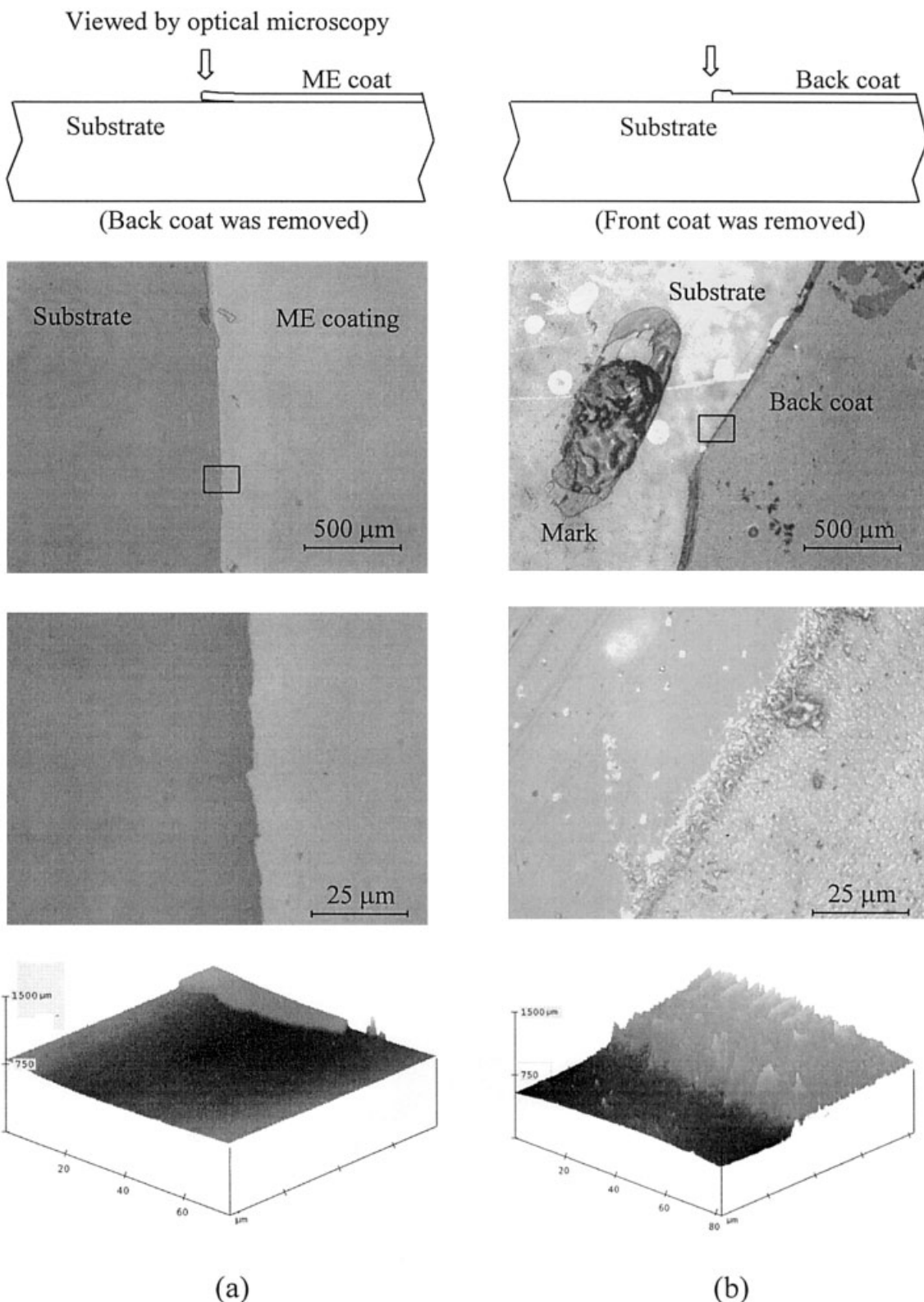


Figure 4 Methodology of measuring the thickness of (a) front coat and (b) back coat of ME-Hi8 tape.

erty of magnetic tape is generally governed by its substrate material.

By comparing the details of loss tangent data for MP-DLT samples in Figure 6(b), it can be seen that the

data for the tape are slightly higher than those for the substrate, covering a wide vertical range as the frequency changes, especially at the temperatures close to the  $T_g$ . This makes the onset temperature [extrapo-

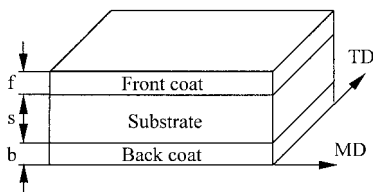


Figure 5 Nomenclature used for rule of mixtures equations.

lation of the loss tangent curve at maximum slope, as shown in Fig. 6(b)] for the MP-DLT tape lower than that for the substrate, although the peak temperatures of the loss tangent for these two samples are still the same. The magnitude of loss tangent for the tape is higher than that for the substrate when the temperature is below the  $T_g$ . Thus, the MP-DLT tape shows slightly higher viscoelastic behavior than that of the substrate. It should be noted that the magnetic tape can be regarded as a multilayer composite, and the energy dissipated during the sinusoidal loading comes not only from its composing materials, but also from the interface.

Figure 6(c) shows the storage moduli and loss tangents for MP-LTO samples. The dynamic mechanical property of magnetic tape is clearly governed by its substrate material, and the tape shows slightly higher viscoelastic property than that of the substrate. By comparing the storage moduli at high frequency and low temperature for MP-DLT and MP-LTO samples in Figure 6(a) and (c), it can be seen that the PEN-based MP-LTO tape has a higher modulus (10–12 GPa) than that of the PET-based MP-DLT tape ( $\sim 9$  GPa). Thus, the PEN-based tape has a better elastic property than that of the PET-based tape at high frequency and low temperature. By comparing the corresponding loss tangent data in Figure 6(b) and (c), it can be seen that the data for MP-DLT samples are lower than that for MP-LTO, which indicates that the PET-based tape has a better viscoelastic property than that of the PEN-based tape.

The statement that the dynamic mechanical property of magnetic tape is governed by its substrate material also applies to the ME-Hi8 sample [Fig. 6(d) and (e)] and the ME-MDV sample [Fig. 6(f)], although the storage moduli for ME tapes were higher than those for the substrate. For ME tapes, there was no obvious difference between the loss tangents for tapes and their substrates.

By comparing the storage moduli data for MP-DLT, MP-LTO, ME-Hi8, and ME-MDV, it can be seen that the storage moduli for MP samples in a wide range of frequencies are higher than those for ME samples. For example, the storage moduli for the MP-DLT tape and substrate at 30°C, 28 Hz are 8.2 and 7.8 GPa, respectively, whereas the corresponding data for ME-Hi8

tape and substrate are 6.9 and 4.9 GPa, respectively. The differences in the moduli of the tapes primarily arise from differences in the moduli of substrates. The selection of the substrate is determined by the tape application. The MP tapes in this study are used in linear drives, whereas the ME tapes are used in rotary drives. In the case of linear drives, high elastic modulus along the longitudinal direction is required for thinner substrates to avoid stretching. In the case of rotary drives, the track is written along an axis at an angle, on the order of 5°, to the tape length. The lateral deformation is more important than the longitudinal direction of the tape in a rotary drive system because the tension in the lateral direction is higher than that in the longitudinal direction. Thus, the substrates for ME tapes are generally “balance” drawn or slightly tensilized along the transverse direction (TD), not like the substrates for MP tapes, which are highly tensilized in the machine direction (MD).

In summary, the dynamic mechanical property of magnetic tape is governed by its substrate material. MP tapes show slightly more viscoelastic behavior than that of their substrates, although there are no obvious differences between the viscoelastic behaviors of ME tapes and their substrates. The PEN-based tapes have good elastic stiffness at high frequency and low temperature, whereas the PET-based tapes have low loss tangents and stable moduli below the  $T_g$  temperature. The substrates for MP tapes were selected to have high moduli along the longitudinal direction, whereas this was not the top priority for the substrate for ME tapes.

#### Master curves of storage modulus

Based on the storage modulus data in Figure 6, master curves of storage modulus for all samples were generated by applying the technique known as frequency/temperature superposition.<sup>16,17</sup> Using this technique, storage moduli measured at the elevated temperatures are superimposed to predict the behavior at longer time periods (lower frequencies) at a reference temperature (30°C). The results are presented in Figure 7. It gives a wide perspective on the storage moduli for the tape, combined layers, and substrates. Moreover, we can have a clear comparison between the substrates and the virgin films, and see the effects of the tape manufacturing process on the storage modulus of substrates.

#### Effect of the tape manufacture processing on the mechanical properties of substrate film

Based on Figure 7 and Table II, it is interesting to see that for all four tapes, none of the substrates showed degradation compared to the virgin film; instead, most of them show strengthened storage moduli. Studies

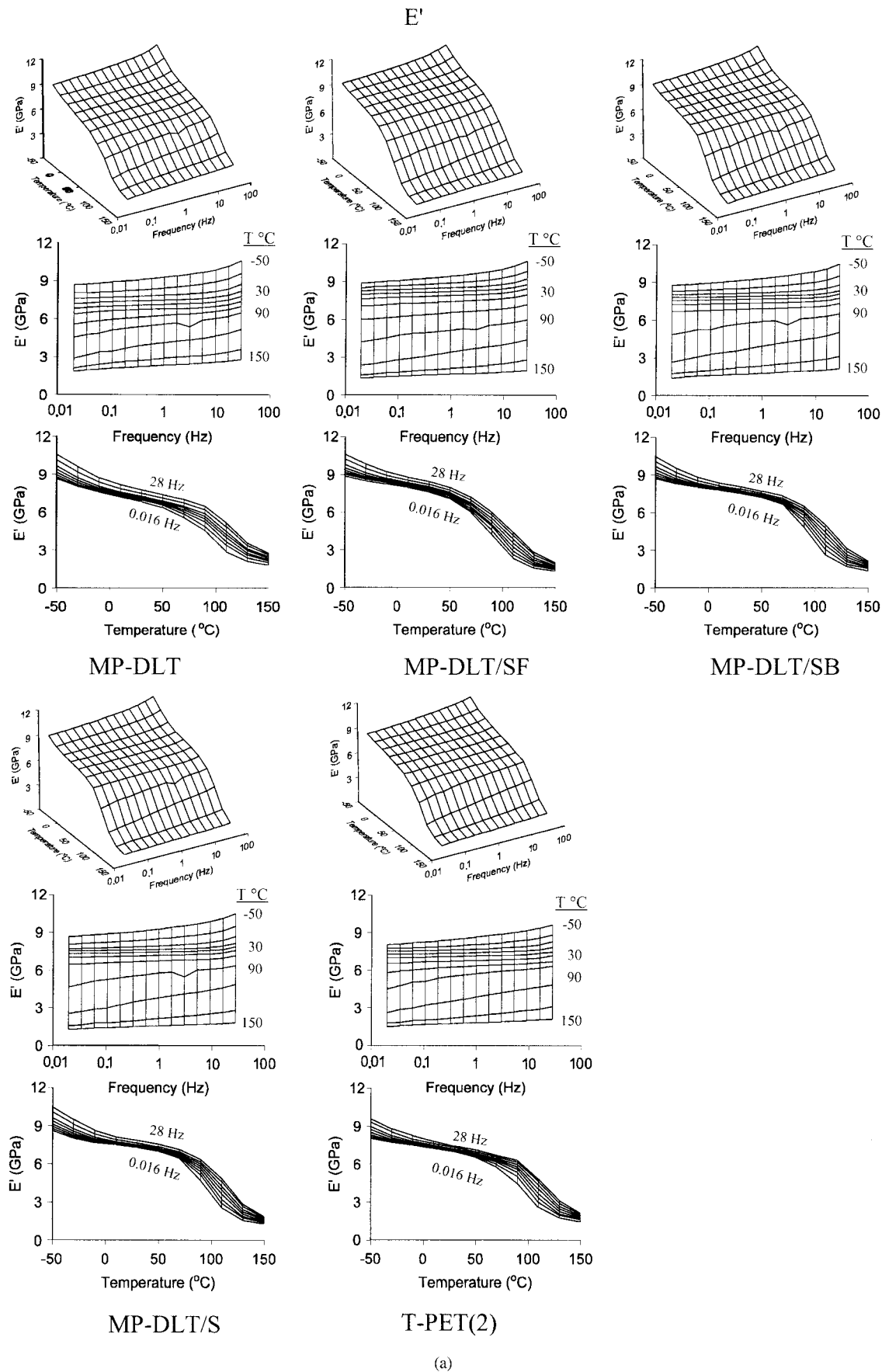


Figure 6 Dynamic mechanical analysis data on (a, b) MP-DLT, (c) MP-LTO, (d, e) ME-Hi8, and (f) ME-MDV.

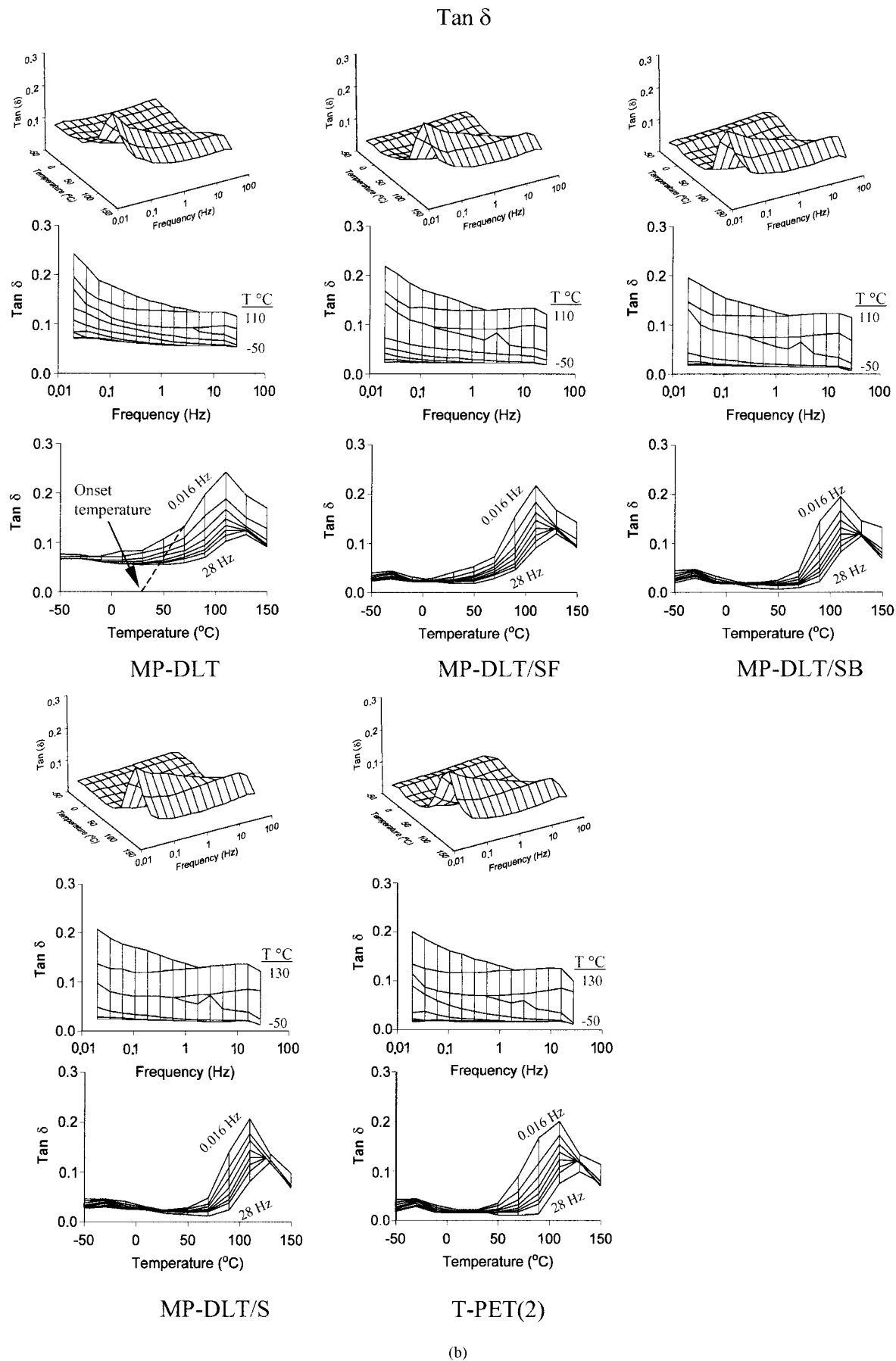


Figure 6 (Continued from the previous page)

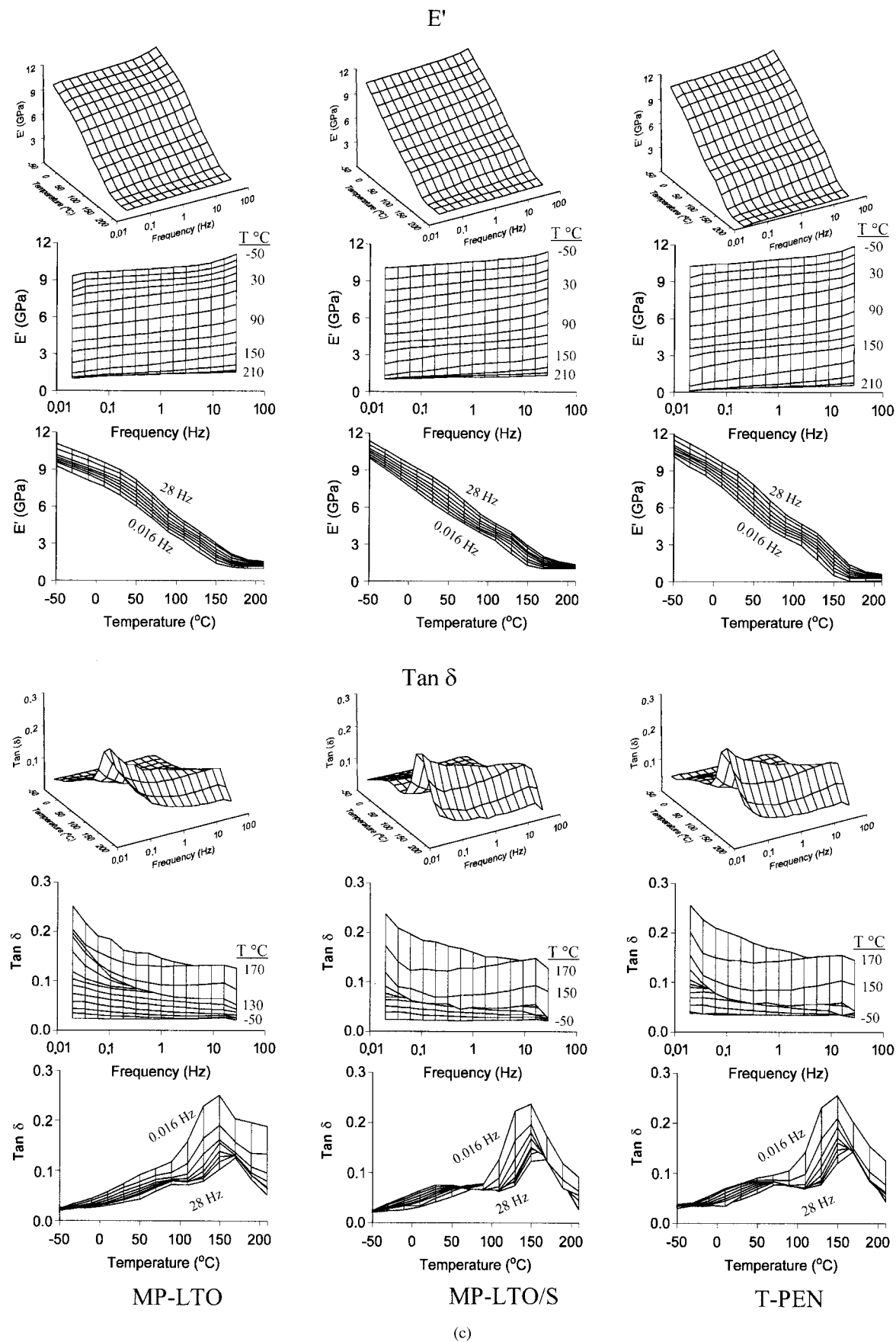


Figure 6 (Continued from the previous page)

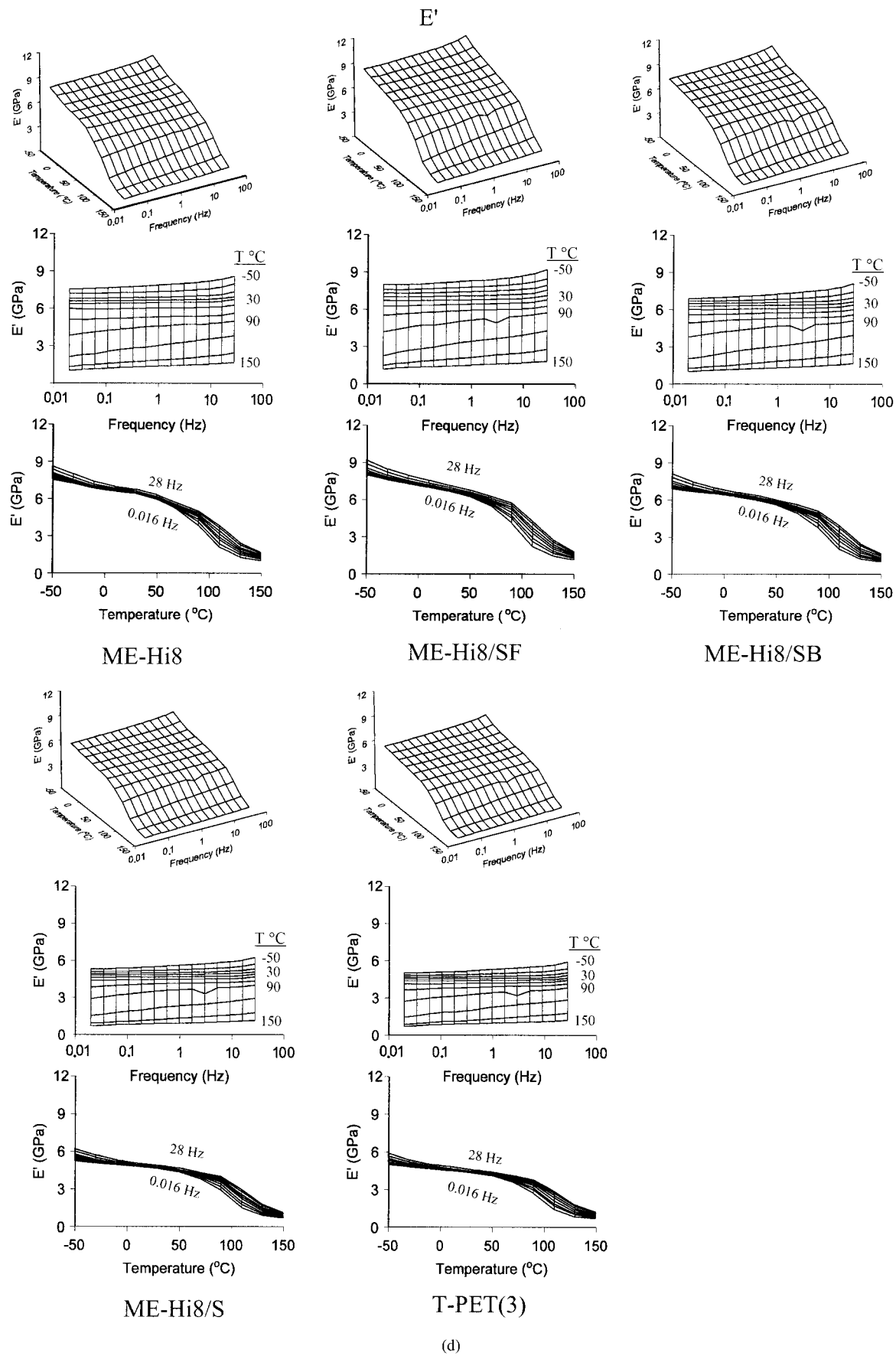
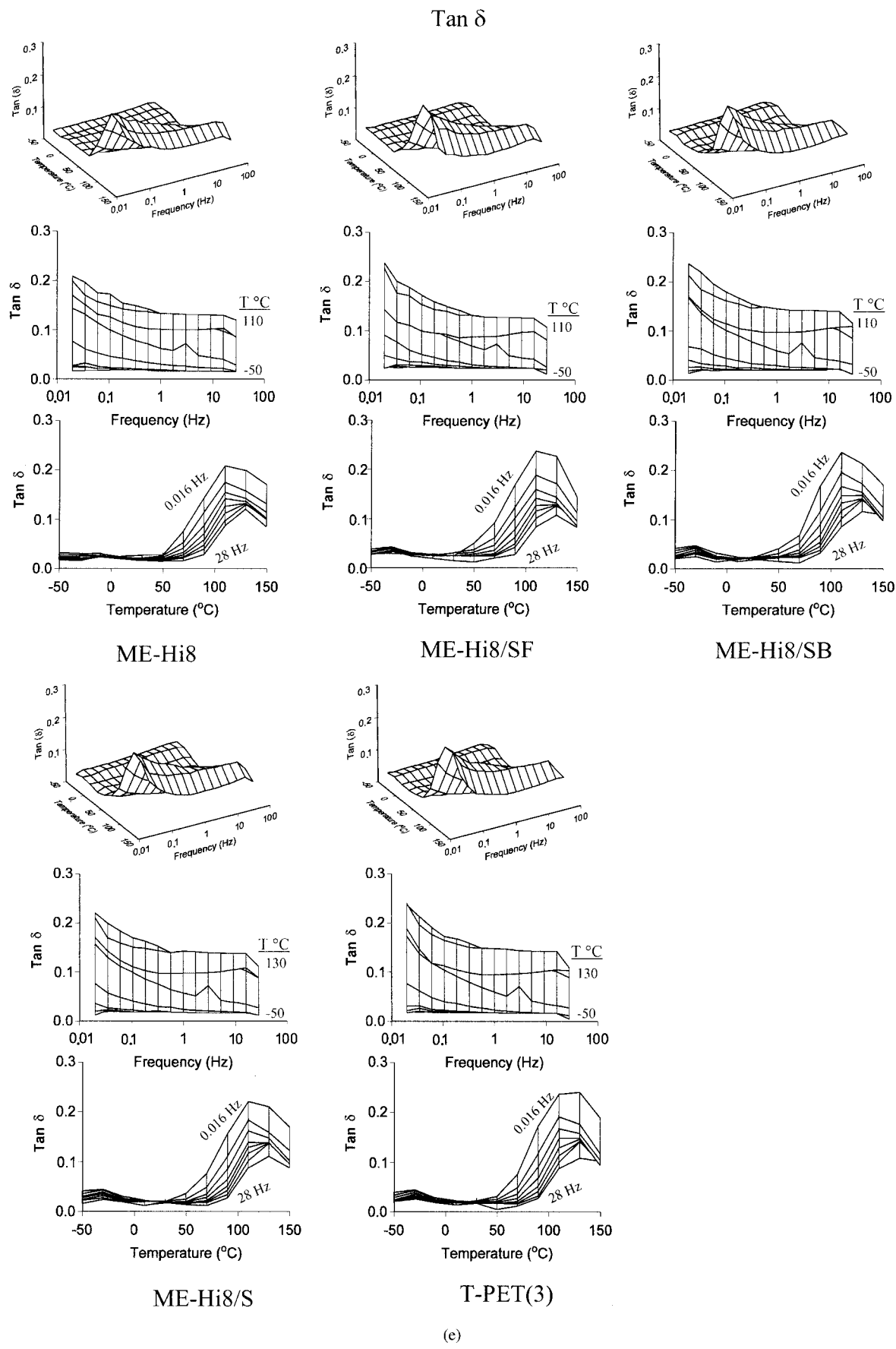


Figure 6 (Continued from the previous page)

**Figure 6** (Continued from the previous page)

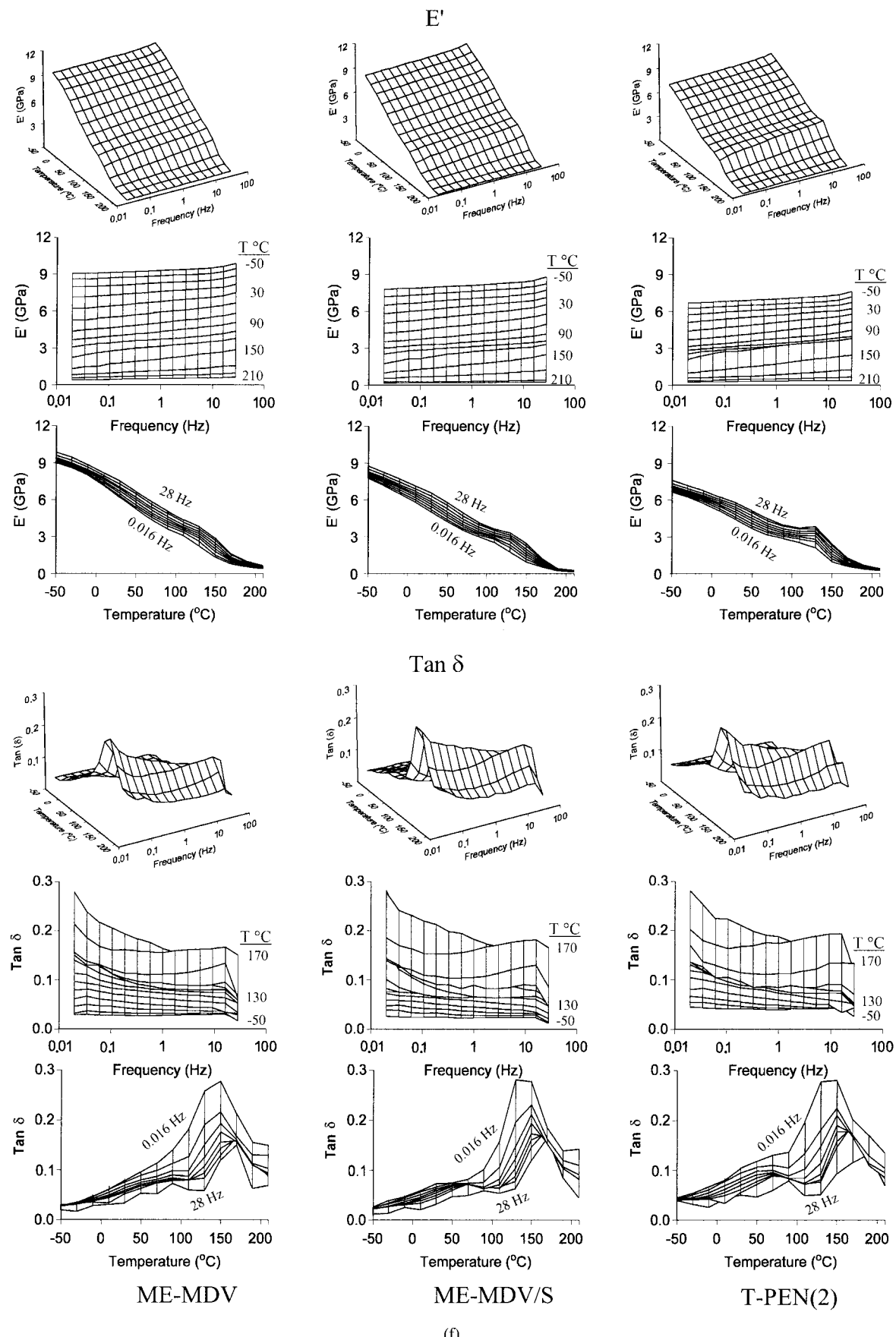


Figure 6 (Continued from the previous page)

**TABLE II**  
**Storage Modulus (GPa) of Various Samples in the Medial Direction at 0.016/28 Hz, 25°C, and 45–55% RH**

Tape	Substrate + front coat	Substrate + back coat	Substrate	Never-coated substrate film
MP-DLT 7.2/8.2	MP-DLT/SF 7.6/8.4	MP-DLT/SB 7.5/8.0	MP-DLT/S 7.3/7.9	T-PET(2) 7.1/7.5
MP-LTO 7.1/9.1			MP-LTO/S 6.5/8.6	T-PEN 6.6/9.0
ME-Hi8 6.4/6.8	ME-Hi8/SF 6.7/7.2	ME-Hi8/SB 6.0/6.4	ME-Hi8/S 4.7/4.9	T-PET(3) 4.4/4.7
ME-MDV 6.3/7.6			ME-MDV/S 5.2/6.7	T-PEN(2) 4.6/5.9

have shown that annealing the polyester film at temperatures below the  $T_g$  does not result in a significant decrease in mechanical properties,<sup>1,18,19</sup> whereas Gillmor and Greener<sup>20</sup> found that annealing treatment on PEN films resulted in lower loss tangent at the  $\alpha$ -relaxation, and a lower decrease in relaxation moduli (moduli at very low deformation frequencies). Previous work in the authors' group also found that lateral

deformation resistance of some tape substrates (PET and PEN) was strengthened compared to that of the virgin films.<sup>10</sup>

All the substrate films used in this study were biaxially oriented, and were metastable in two respects. First, the percent crystallinity of the film was much lower than the equilibrium crystallinity content. When the temperature is high, the molecular segments in the

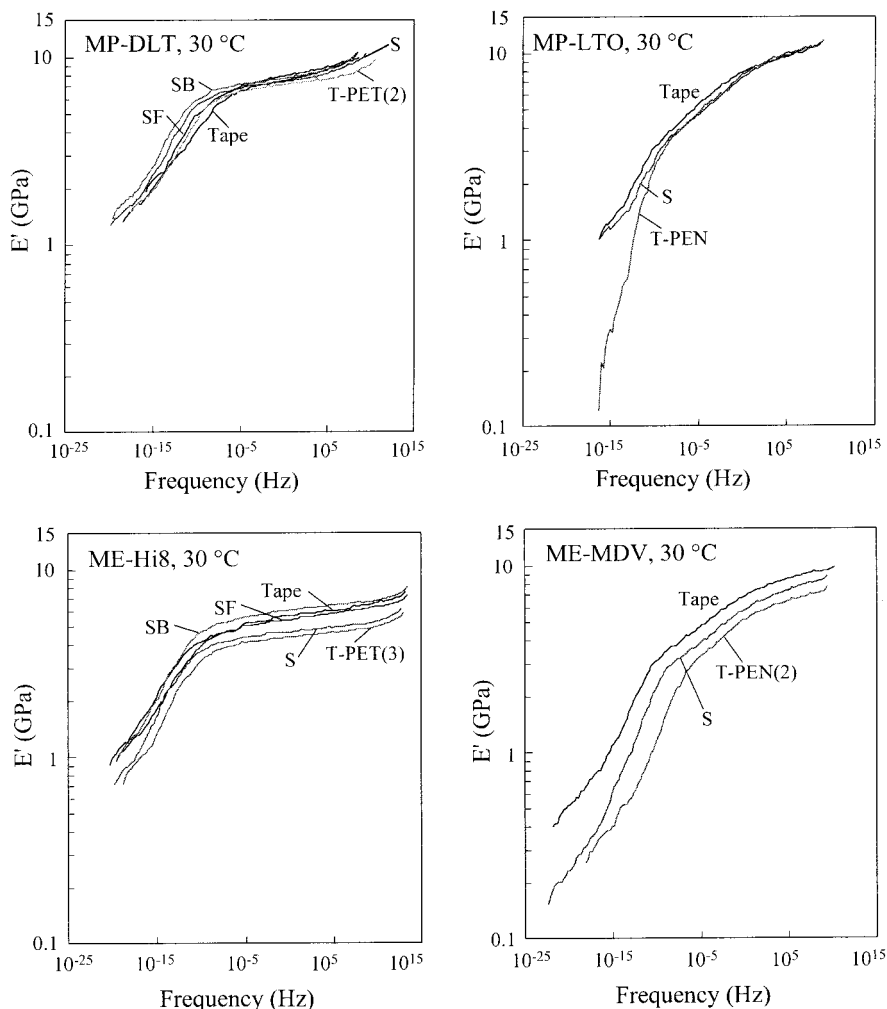


**Figure 7** Master curves of storage modulus ( $E'$ ) of various tapes and their layers at 30°C. (a) MP-DLT, (b) MP-LTO, (c) ME-Hi8, (d) ME-MDV.

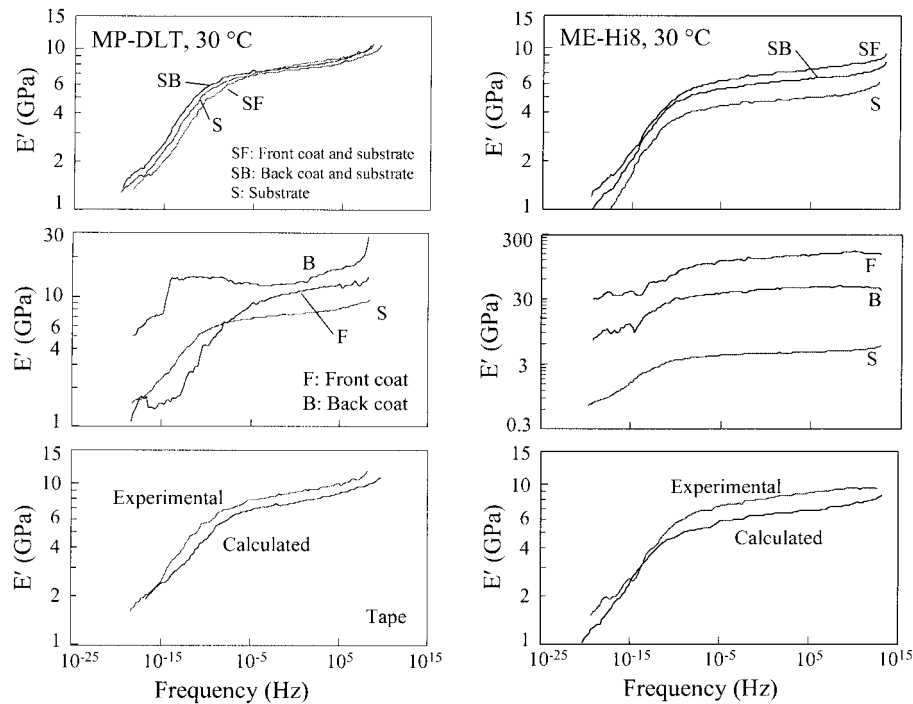


**Figure 8** Master curves of storage moduli for MP-DLT and ME-Hi8 samples at 30°C, showing the experimental and calculated data for front and back coats determined by using the rule of mixtures, and comparison of experimental and calculated moduli for the tape.

amorphous region tend to move and form oriented chains or even crystallize to reduce the system entropy. High crystallinity results in high mechanical properties. Second, amorphous regions of the film contained a frozen-in strain, which tended to relax and to make the film contract.<sup>1</sup> Annealing at temperatures below the  $T_g$ , which occurs during the tape manufacturing, helped to thermal-set the film and increase the dimensional stability.

On the other hand, when the temperature is higher than the glass-transition temperature, the main chain of the polymer film molecules will have enough energy to move and rotate. As a result, the biaxially oriented structure could be significantly affected. The mechanisms of thermal degradation include the residual stress relaxation, molecule segments recoiling, and selected-chain scission or random-chain scission.<sup>21</sup> Stress relaxation also reduces the anisotropy of the film's mechanical properties. This effect is, obviously, more significant for the films that are highly tensilized in one direction, say MD. Because the MP-DLT and MP-LTO tapes are used for linear drives, the substrates T-PET(2) and T-PEN are more stretched in MD than in TD. Thus the effect of strengthening and weakening of the MP tape manufacturing process seems to counteract the effect, and there is almost no change to the storage moduli between the substrates and the virgin films. In the case of ME tapes, the balance-drawn films were less affected by the residual stress relaxation than those tensilized films used for MP

tapes. Thus, both the ME tape substrates showed strengthening compared to the virgin films. The reason that the T-PEN(2) film showed more strengthening than T-PET(3) film (Fig. 7) comes from the fact that PEN films contain more amorphous regions, and have a larger driving force for stress relaxation and recrystallization at elevated temperature than that of PET films. This is consistent with the study on their lateral deformation behavior by the laser scanning microscopy (LSM) technique.<sup>10</sup> In that work, the samples were loaded at 25°C, 50% RH, and 7 MPa external stress for 12 min. The longitudinal and lateral deformations for ME-MDV/S were 0.173 and 0.035%, respectively, lower than those for the virgin film T-PEN(2), which were 0.191 and 0.039%, respectively.

#### Calculation of mechanical properties of individual layers

By applying the rule of mixtures to the data of substrate and combined layers (substrate plus front coat or substrate plus back coat), the mechanical properties of the individual layers, say front coat or back coat, can be calculated.

Figure 8 shows the predicted storage modulus curves for MP-DLT and ME-Hi8 samples. The left top panel of Figure 8 shows the storage moduli of substrate and its combination with front or back coats; the left middle panel shows the calculated storage moduli for front coat and back coat; and the left bottom panel

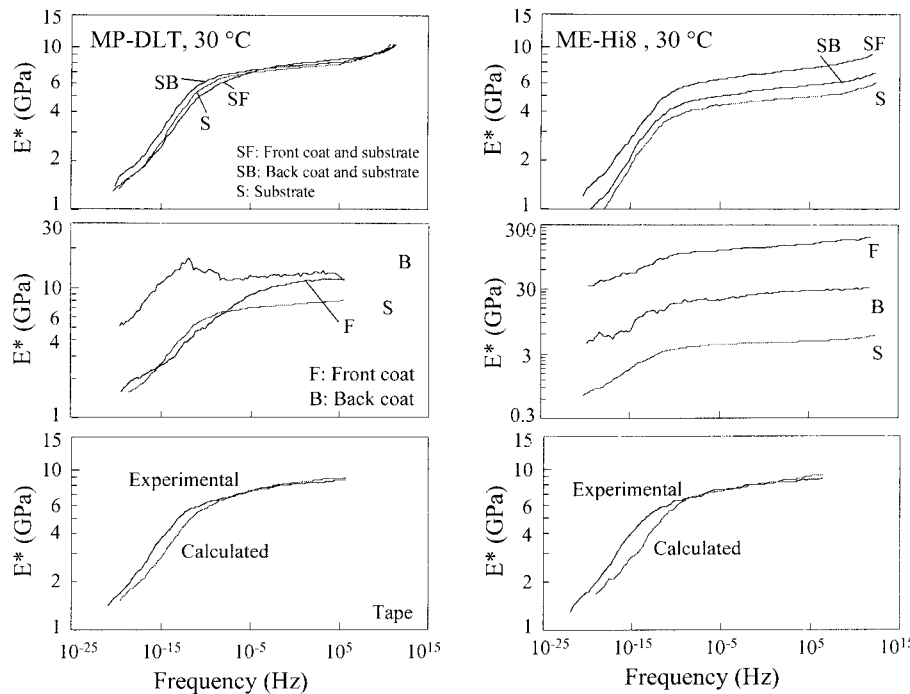


Figure 9 Master curves of complex moduli for MP-DLT and ME-Hi8 samples at 30°C.

shows the storage moduli for the finished tape, all calculated by using the rule of mixtures approach and from the experimental measurement. The right panels of Figure 8 show the results on ME-Hi8 samples.

Both the front and back coats in the MP-DLT tape had higher storage moduli than that of the substrate. The back coat showed a constant modulus over a wide frequency range, which was not seen for other materials in this study. The abnormally high values for the back coat at about  $10^{-15}$  Hz may arise from the measurement error. The behavior of the substrate at this frequency was comparable to its behavior at the temperature around  $T_g$ . The increased deformability of the substrate may have affected the accurate DMA measurement on the combined layers. The calculation results for ME-Hi8 samples show that the front coat has a significantly higher storage modulus, on the order of 100–200 GPa. The numbers may contain some error, arising from the error in the coating thickness measurement, the process of coating removal on the property of the remaining layer, and the DMA test. However, it is reasonable that the front coat had a much higher storage modulus than that of the substrate, given that the front coat contains a DLC coating, which is supposed to have extremely high stiffness.

In the left bottom panel of Figure 8, the calculated storage moduli for the MP-DLT tape are slightly lower than the experimental values. As we discussed above, the energy dissipation of the magnetic tape comes not only from its various layers, but also from the interface. In the rule of mixtures, the interface is assumed to be ideal, that is, there is no energy dissipation or

viscoelastic behavior across the interface; this is not true for the magnetic tapes.

It will be shown later that for the calculation of CTE for the individual layers, we would need complex moduli for the various samples. Figure 9 shows the rule of mixtures approach for individual layers on the behavior of complex modulus. The figure shows features similar to those in Figure 8, except the calculated values for the finished MP-DLT and ME-Hi8 tapes have good match with the experimental results. Only a small deviation at very low frequencies (lower than  $10^{-10}$  Hz) exists, which is believed to be attributable to the error in the DMA measurement at high temperatures, above the  $T_g$  of the substrate.

#### Summary of the mechanical properties for tapes samples

Figure 10(a) summarizes the storage moduli of various samples at 0.016 and 28 Hz at 25°C; the data are linearly interpolated from the storage moduli data at 10 and 30°C from the DMA test. To compare with other relevant mechanical properties, Figure 10(b)–(d) show the Poisson's ratio, longitudinal elongation, lateral contraction, and lateral creep for the various samples measured using the LSM technique.<sup>10</sup> In both Figure 10(a) and (b), tapes show properties similar to those of their substrates. The storage moduli for the PEN-based tapes MP-LTO and ME-MDV increase significantly as the deformation frequency increases,

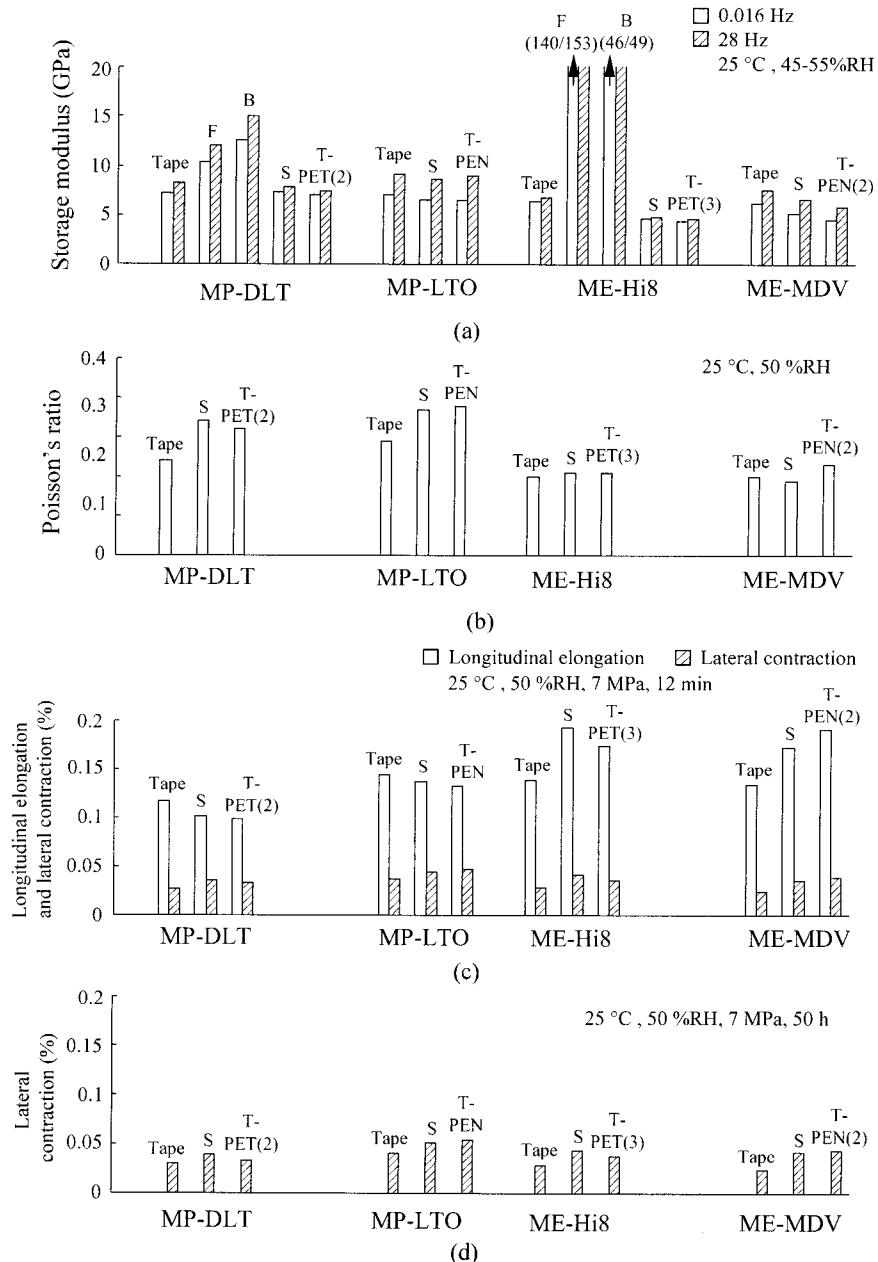


**Figure 10** Summary of the elastic and viscoelastic properties for various samples. (a) Storage moduli; data for the front and back coats are calculated, and all the others are measured. The reproducibility for the DMA measurement is about  $\pm 5\%$ . (b) Poisson's ratio; the error is about  $\pm 5\%$ .<sup>9,10</sup> (c) Longitudinal elongation and lateral contraction for various samples at 25°C, 50% RH, 7 MPa uniaxial stress for 12 min. The reproducibility for the measurement is about  $\pm 5\%$ .<sup>10</sup> (d) Lateral contraction at 25°C, 50% RH, 7 MPa uniaxial stress for 50 h.<sup>10</sup>

which are identical to the storage moduli as a function of deformation frequency for PEN substrates in both this work and previous DMA study.<sup>8</sup> Poisson's ratios for the ME tapes ME-Hi8 and ME-MDV were around 0.20, very close to those for the corresponding substrates, T-PET(3) and T-PEN(2). Poisson's ratios for MP tapes are slightly lower than those for their substrates. The viscoelastic properties in Figure 10(c) are slightly different from the elastic properties in Figure 10(a). The MP-DLT/S, MP-LTO/S, and ME-Hi8/S

show slightly weakened viscoelastic properties compared to those of the virgin films, whereas there is either no change or slight strengthening in elastic moduli. However, the ME-MDV/S shows obvious strengthening compared to T-PEN(2), and this is the same as that in the elastic storage moduli in Figure 10(a). The lateral creep data in Figure 10(d) show similar results with those in Figure 10(c); generally, at current test conditions, ME tapes exhibit less lateral contraction than that of MP tapes.

TABLE III  
Summary of the Coefficient of Thermal Expansion  
( $\times 10^{-6}/^{\circ}\text{C}$ ) Data at Ambient (Uncontrolled)  
Humidity Using TMA<sup>a</sup>

Tape	Direction <sup>b</sup>	Temperature (°C)			
		30–40	40–50	50–60	60–70
MP-DLT	MD	3.8	5.6	3.1	-7.9
	TD	12.9	16.8	19.5	23.8
MP-DLT/SF	MD	2.0	5.4	2.4	-7.5
	TD	11.9	15.9	21.5	29.6
MP-DLT/SB	MD	-1.3	0.2	1.1	-1.4
	TD	11.7	17.3	22.9	24.3
MP-DLT/S	MD	-2.6	-1.9	-1.1	-2.5
	TD	12.6	16.2	22.3	26.2
T-PET(2)	MD	-4.5	-0.4	1.9	2.0
	TD	1.9	14.2	20.9	25.7
MP-LTO	MD	1.8	3.9	1.6	-2.3
	TD	5.3	8.6	12.5	16.4
MP-LTO/S	MD	-3.5	0.3	1.2	-0.2
	TD	1.4	11.0	13.9	17.4
T-PEN	MD	-6.3	0.9	5.8	8.3
	TD	2.5	7.8	11.5	14.6
ME-Hi8	MD	9.9	13.9	15.4	13.7
ME-Hi8/SF	MD	12.1	14.8	15.2	17.4
ME-Hi8/SB	MD	14.8	17.4	18.1	16.2
ME-Hi8/S	MD	13.5	16.4	18.8	15.7
T-PET(3)	MD	14.3	17.6	23.3	21.2
	TD	5.1	8.9	12.2	16.3
ME-MDV	MD	9.9	13.8	15.4	13.7
ME-MDV/S	MD	12.3	17.1	20.8	17.3
T-PEN(2)	MD	12.4	18.6	26.6	21.8
	TD	-8.4	-5.3	-1.9	-0.2

<sup>a</sup> From Md and Bhushan.<sup>10</sup>

<sup>b</sup> MD, medial direction; TD, transverse direction.

### Thermal expansion results

The CTE data measured by TMA are summarized in Table III. By applying the rule of mixtures, the CTE of individual layers can be calculated from the data of combined layers. A model was proposed in previous work to calculate the CTE of individual layers of magnetic tapes.<sup>10</sup> However, this model can be realized only when the moduli of various samples at elevated temperatures are available, such as in this work from the DMA test. With reference to Figure 11, the original linear dimension of the combined layer structure is one ( $x_0 = 1$ ). After a unit temperature increase ( $\Delta T = 1$ ), the structure expands by  $\Delta x_{sf}$ . Assuming that the thermal expansions of the tape samples along MD and TD are independent, the dimension and stress condition in TD are not considered in this work. If there were not interfacial bonding, the free thermal expansion of the substrate after the temperature increase would be  $\Delta x_s$ , whereas that of the front layer would be  $\Delta x_f$ . Thus, there would be an interfacial shear stress that causes a ( $\Delta x_{sf} - \Delta x_s$ ) deformation in the substrate and a ( $\Delta x_{sf} - \Delta x_f$ ) deformation in the front layer. That is,

$$\sigma = (\Delta x_{sf} - \Delta x_f)E_f f = -(\Delta x_{sf} - \Delta x_s)E_s s \quad (10)$$

TABLE IV  
Complex Moduli of Various Samples in the Machine  
Direction at 0.016 Hz, Different Temperatures (GPa),  
and 45–55% RH

Tape	Temperature (°C)			
	35	45	55	65
MP-DLT	7.86	7.62	7.21	6.64
MP-DLT/SF	7.49	7.23	6.83	6.29
MP-DLT/SB	6.40	6.95	7.09	6.82
MP-DLT/S	7.22	7.07	6.86	6.59
MP-DLT/F	10.2	10.0	9.17	7.68
MP-DLT/B	12.6	12.5	12.2	11.7
ME-Hi8	7.80	7.51	7.11	6.61
ME-Hi8/SF	6.66	6.43	6.13	5.76
ME-Hi8/SB	5.25	5.07	4.83	4.53
ME-Hi8/S	4.57	4.48	4.28	3.98
ME-Hi8/F	175	165	152	135
ME-Hi8/B	30.9	30.8	28.4	23.7

Given that  $\Delta x_s = \alpha_s x_0 \Delta T$ , we have

$$E_f f (\alpha_{sf} - \alpha_f) = E_s s (\alpha_s - \alpha_{sf}) \quad (11)$$

where  $\alpha_s$ ,  $\alpha_f$ , and  $\alpha_{sf}$  are the CTE of the substrate, front coat, and the composite, respectively. Thus, we have

$$(E_f f + E_s s) \alpha_{sf} = E_f f \alpha_f + E_s s \alpha_s \quad (12)$$

By considering eq. (9), we finally get

$$E_{sf} (f + s) \alpha_{sf} = E_f f \alpha_f + E_s s \alpha_s \quad (13)$$

If  $E_{sf}$ ,  $f$ ,  $s$ ,  $\alpha_{sf}$ ,  $E_f$ ,  $\alpha_f$ ,  $E_s$ , and  $\alpha_s$  are known, we can calculate  $\alpha_f$ , the CTE of the front coat layer and, similarly, the CTE of the back coat.

The rule of mixtures is based on an "isostain" assumption. For a composite during thermal expansion, the strain includes both elastic and viscoelastic parts. Thus, the complex modulus instead of storage modulus is used in the rule of mixtures to calculate the CTE of the individual layers. Table IV lists the complex moduli of the corresponding layers. The data for tape, substrate, and combined layers are obtained

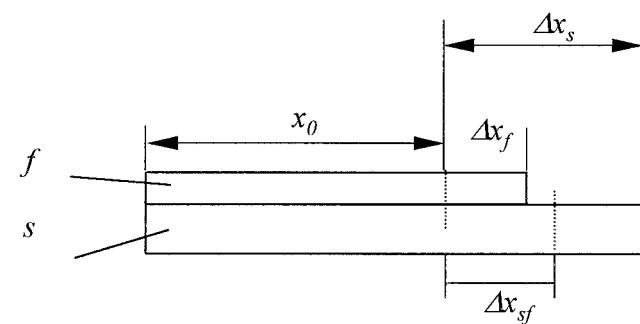


Figure 11 Schematic of the two-layer composite after thermal expansion.

TABLE V  
Calculated Coefficient of Thermal Expansion ( $\times 10^{-6}/^{\circ}\text{C}$ )  
of Individual Layers and the Tape in the Machine  
Direction at Ambient (Uncontrolled) Humidity

Tape	Temperature ( $^{\circ}\text{C}$ )			
	30–40	40–50	50–60	60–70
MP-DLT/F	9.9	17.2	8.4	-16.3
MP-DLT/B	12.0	18.2	19.8	8.2
MP-DLT/S	-2.6	-1.9	-1.1	-2.5
MP-DLT	2.7	6.2	3.7	-6.1
MP-DLT <sup>a</sup>	3.8	5.6	3.1	-7.9
ME-Hi8/F	7.1	8.7	5.8	17.9
ME-Hi8/B	15.3	14.8	9.2	14.5
ME-Hi8/S	13.5	16.4	18.8	15.7
ME-Hi8	12.3	14.5	14.0	16.6
ME-Hi8 <sup>a</sup>	9.9	13.9	15.4	13.7

<sup>a</sup> Indicates the experimental data.

from the complex moduli of corresponding material at 0.016 Hz, and 30, 50, and 70°C. The data for front and back coats are calculated values. By applying the data in Tables III and IV into eq. (13), the CTE of the front and back coats of MP-DLT and ME-Hi8 were calculated and are listed in Table V. The data are on the same order as those of the substrate, whereas the CTE for the front coats is lower than that for the back coats, for both MP and ME tapes. In MP-DLT samples, the CTE of the substrate is negative all through the 30–70°C temperature range, showing that T-PET(3) has large residual stress, which continues to relax during the heating. The CTE for the front coat shows a sudden shrinkage at high temperature (60–70°C).

Considering the stable data of the substrate and back coat, it is reasonable to believe that the shrinkage of the tape at 60–70°C is contributed by the front coat. In the ME-Hi8 sample, all the layers and the tape show constant positive CTE through the testing temperature range, which indicates that the residual stress along the MD does not exist in any layers of this tape.

To verify this approach, the CTE of the tape as a composite of front coat, substrate, and back coat was also calculated using the rule of mixtures, as follows:

$$E_{\text{tape}}(f + s + b)\alpha_{\text{tape}} = E_f f \alpha_f + E_s s \alpha_s + E_b b \alpha_b \quad (14)$$

where  $E_{\text{tape}}$  and  $\alpha_{\text{tape}}$  are the complex and CTE for the finished tape, respectively. The results are also listed in Table V. The calculated CTE values of MP-DLT and ME-Hi8 match the experimental values well.

The CTE values for various samples are summarized in Figure 12. The coefficient of hygroscopic expansion (CHE) data from Ma and Bhushan<sup>10</sup> are also included for comparison. Table VI also summarizes CTE and CHE data along with mechanical properties data presented in Figure 10. It is clear that the properties of magnetic tapes are governed by their substrates. MP tapes use highly tensilized substrates, which have negative CTE in MD; as a result, the CTE values for MP tapes are significantly lower than those for ME tapes, which use balance-drawn substrates. The CHE values for MP tapes and substrates were higher than those for ME tapes and substrates. By applying the rule of mixtures, one may also obtain the CHE for the individual layers of magnetic tapes, although it requires the moduli of the sample at various relative humidities, which requires further investigation.

## CONCLUSIONS

The dynamic mechanical properties of magnetic tapes are generally governed by their substrate materials. MP tapes show slightly more viscoelastic behavior than that of their corresponding substrates, although there are no obvious differences between the viscoelastic behavior of ME tapes and their substrates. The PEN-based tapes have good elastic stiffness at high frequency and low temperature, whereas the PET-based tapes have low loss tangents and stable moduli below the  $T_g$  temperature. The storage moduli for MP tapes and substrates are higher than those for ME tapes and substrates along the longitudinal direction; this is because the substrates are selected according to the requirement for the linear and helical drive systems, in which MP and ME tapes are used.

None of the substrates for the four tapes showed mechanical degradation after the tape manufacturing process. The storage moduli for the substrates of ME tapes are higher than those for the virgin films, believed to be attrib-

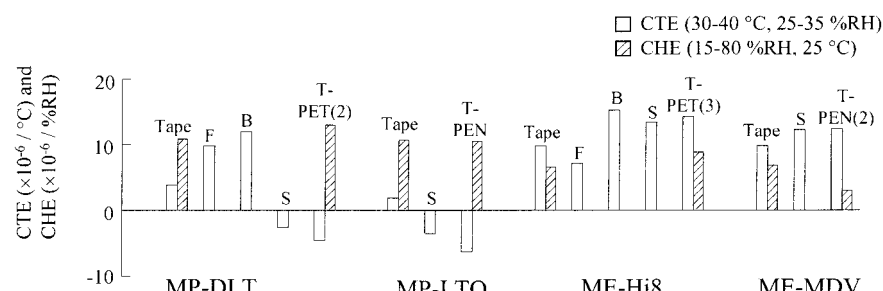


Figure 12 Summary of the CTE and CHE for various samples. The error for CTE is about  $\pm 1.5 \times 10^{-6}/^{\circ}\text{C}$ , and the error for CHE is about  $0.5 \times 10^{-6}/\%$  RH.<sup>9</sup>

**TABLE VI**  
**Summary of the Properties for Various Samples in the Machine Direction**

	CTE ( $\times 10^{-6}$ / °C) at 25–35% RH (30–40°C)	CHE ( $\times 10^{-6}$ / % RH) at 25°C (15–80% RH)	$E'$ (GPa) at 25°C, 45–55% RH		Poisson's ratio <sup>a,b</sup>	Longitudinal elongation <sup>a</sup> (%) 12 min	Lateral contraction <sup>a</sup> (%)	
			0.016 Hz	28 Hz			12 min	50 h
MP-DLT	3.8	10.9	7.2	8.2	0.24	0.117	0.027	0.031
MP-DLT/F	9.9		10.3	12.0				
MP-DLT/B	12.0		12.6	15.0				
MP-DLT/S	−2.6		7.3	7.9	0.34	0.101	0.036	0.040
T-PET(2)	−4.5	13.0	7.1	7.5	0.32	0.099	0.033	0.034
MP-LTO	1.8	10.7	7.1	9.1	0.29	0.145	0.037	0.041
MP-LTO/S	−3.5		6.5	8.6	0.37	0.137	0.045	0.052
T-PEN	−6.3	10.6	6.6	9.0	0.38	0.133	0.047	0.055
ME-Hi8	9.9	6.6	6.4	6.8	0.20	0.138	0.028	0.029
ME-Hi8/F	7.1		140	153				
ME-Hi8/B	15.3		46	49				
ME-Hi8/S	13.5		4.7	4.9	0.21	0.193	0.042	0.044
T-PET(3)	14.3	8.9	4.4	4.7	0.21	0.174	0.035	0.038
ME-MDV	9.9	6.9	6.3	7.6	0.20	0.134	0.024	0.025
ME-MDV/S	12.3		5.2	6.7	0.19	0.173	0.035	0.042
T-PEN(2)	12.4	3.0	4.6	5.9	0.23	0.191	0.039	0.044

<sup>a</sup> Testing conditions: 25°C, 50% RH.

<sup>b</sup> Measured at a stress range from 5 to 40 MPa, stress step of 7 MPa, and time interval of 12 min.

utable to the thermal-setting effect of the tape manufacturing process. T-PEN(2) film shows more strengthening than T-PET(3) film after ME tape manufacturing because the PEN film contains a greater amorphous region, and is more affected by thermal setting than is the PET film.

The storage and complex moduli of the front and back coats of MP and ME tapes were calculated by the rule of mixtures. Both the front and back coats of the MP-DLT tape were found to be slightly stiffer than their substrates. Frequency/temperature superposition was used to obtain the data at a wide range of frequencies. The back coat had a constant modulus over a wide frequency range from  $10^{-10}$  to  $10^{10}$  Hz. The modulus for the front coat for ME-Hi8 was on the order of 100–200 GPa, and the modulus for the back coat was also higher than that for the substrate. The calculated complex moduli for finished tapes show good match with the experimental data.

Based on the CTE and complex moduli data of the tapes, substrates, and combined layers, the CTE for the individual layers of the four tapes were calculated. The model provides a good match between the predicted CTE values for the finished tapes and the experimental data. The CTE values for the front coats of both MP-DLT and ME-Hi8 were lower than the CTE values for the corresponding back coats. The thermal shrinkage of the MP-DLT tape at 60–70°C is believed to result from the shrinkage of the front coat at this temperature range. There was no thermal shrinkage for the ME-Hi8 samples through the testing temperatures. The CHE for MP tape samples was higher than that for ME tape samples.

The research reported in this study was supported by the industrial membership of Nanotribology Laboratory for In-

formation Storage and MEMS/NEMS (NLIM) at The Ohio State University. The authors thank Hideaki Watanabe and Hirofumi Murooka from Teijin-DuPont Ltd. Japan, and Toshifumi Osawa from DuPont-Teijin Ltd., for their generous support and samples: MP-DLT (Fuji), MP-LTO (IBM), ME-Hi8 (Sony), and ME-MiniDV (Panasonic).

## References

1. Bhushan, B. Mechanics and Reliability of Flexible Magnetic Media, 2nd ed.; Springer-Verlag: New York, 2000.
2. <http://www.lto-technology.com/newsite/html/format.html>.
3. Bhushan, B. Tribology and Mechanics of Magnetic Storage Devices, 2nd ed.; Springer-Verlag: New York, 1996.
4. Bobji, M.; Bhushan, B. J Mater Res 2001, 16, 844.
5. Weick, B. L.; Bhushan, B. J Info Storage Proc Syst 2000, 2, 207.
6. Weick, B. L.; Bhushan, B. J Appl Polym Sci 2001, 81, 1142.
7. Higashioji, T.; Bhushan, B. J Appl Polym Sci 2002, 84, 1477.
8. Bhushan, B.; Ma, T.; Higashioji, T. J Appl Polym Sci 2002, 83, 2225.
9. Ma, T.; Bhushan, B.; Murooka, H.; Kobayashi, I.; Osawa, T. Rev Sci Inst 2002, 73, 1813.
10. Ma, T.; Bhushan, B. J Appl Polym Sci, to appear.
11. Chen, D.; Zachmann, H. G. Polymer 1991, 32, 1612.
12. Owners Manual for the Rheometrics RSA-II Dynamic Mechanical Analyzer, Rheometrics: Piscataway, NJ.
13. Storer, R. A. Annu Book ASTM Stand 1997, 14.02, 348–351; 1999, 8.02, 85–88.
14. Bhushan, B. Handbook of Micro/Nanotribology, 2nd ed.; CRC Press: Boca Raton, FL, 1999.
15. Jones, R. M. Mechanics of Composite Materials, 2nd ed.; Taylor & Francis: Philadelphia, 1999.
16. Ward, I. M. An Introduction to the Mechanical Properties of Solid Polymers; Wiley: New York, 1993.
17. Ferry, J. D. Viscoelastic Properties of Polymers, 3rd ed.; Wiley: New York, 1980.
18. Silva, M.; Spinace, M.; Paoli, M. J Appl Polym Sci 2001, 80, 20.
19. Haghishat, M. K.; Borhani, S. J Appl Polym Sci 2000, 78, 1923.
20. Gillmor, J. R.; Greener, J. ANTEC 1997, 45, 1582.
21. Kumar, S. G.; Kumar, R. V.; Madras, G. J Appl Polym Sci 2002, 84, 681.